



1

1 **Decadal trends in observed surface solar radiation and their**
2 **causes in Brazil in the first two decades of the 21st century.**
3

4 Lucas Ferreira Correa¹, Doris Folini¹, Borianna Chtirkova¹, and Martin Wild¹

5 ¹Institute for Atmospheric and Climate Sciences, ETH Zurich, Zurich, Switzerland.

6 *Correspondence to:* Lucas Ferreira Correa (lucas.ferreira@env.ethz.ch)

7 **Abstract.** Numerous studies have investigated the long term variability of surface solar radiation
8 (SSR) around the world. However, the large disparity in the availability of observational data between
9 developed and least developed/developing countries leads to an underrepresentation of studies on SSR
10 changes in the latter. This is especially true for South America, where few observational studies have
11 investigated the SSR decadal trends, and usually only at a local or regional scale. In this study we use
12 data from 34 stations distributed throughout all the regions of Brazil to present the decadal SSR
13 decadal trends in the first two decades of the 21st century and investigate their associated causes. The
14 stations were grouped into 8 composites according to their proximity. Our results show that in the
15 North and Northeast Brazil a strong dimming occurred, with significant contributions from increasing
16 atmospheric absorption, most likely due to anthropogenic emissions, and increasing cloud cover. In
17 the Southeast and Midwest regions of Brazil near-zero trends resulted from competing effects of
18 clear-sky processes and strong negative trends in cloud cover. In the South part of the Amazon and in
19 Southern Brazil a statistically insignificant brightening was observed, with significant contribution
20 from decreasing biomass burning emissions in the former and competing minor contributions in the
21 latter. These results can contribute to deepen the knowledge and understanding of SSR decadal trends
22 and their causes in South America, reducing the underrepresentation of this continent when compared
23 to regions like Europe.

24 **1. Introduction**

25 Decadal trends in surface solar radiation (SSR) have been the object of study since pioneering
26 studies in late 1980s and early 1990s presented evidence that SSR is not constant over time, but rather
27 undergoes decadal trends (Ohmura and Lang, 1989; Russak, 1990; Dutton et al., 1991; Stanhill and
28 Moreshet, 1992). Several studies have followed presenting the trends and discussing their causes and
29 potential consequences in several parts of the world (Wild, 2009). Global dimming (negative trends in
30 SSR) and brightening (positive trends in SSR) have been associated, in most of the cases, with
31 changes in cloud cover (e.g. Stjern et al., 2008; Augustine and Capotondi, 2022) and changes in
32 aerosol loadings (e.g. Wild et al., 202, Kambezidis et al., 2012), with the dominant aspect depending
33 on regional atmospheric and emission features. However, many regions of the world are still
34 underrepresented by such studies, mostly because of the lack of observational high quality data in
35 most of developing and least developed countries in contrast to regions like Europe, North America or
36 Eastern Asia. South America is an important region to be mentioned in this context.



37 The lack of long-term SSR data in South America, reported by different authors (Ohmura,
38 2009; Gilgen et al., 2009), is the main cause for the absence of a long literature in the region. Still, a
39 few studies tried to assess SSR variability in South America. Ohmura (2009) presented and discussed
40 SSR decadal trends based on a few stations in Venezuela. Schwartz (2005) used astronomical
41 extinction measurements to estimate clear-sky SSR trends at one astronomical observatory in Chile.
42 Yuan et al. (2021) used machine learning methods to spatially interpolate SSR ground observations
43 and used this approach to assess SSR decadal variability over the whole globe, including South
44 America. Da Silva et al. (2010), de Jong et al. (2019) and de Lima et al. (2019) all assessed SSR
45 variability in Brazil with a focus on the potential for photovoltaic energy production. Zuluaga et al.
46 (2021) and Raichijik (2012) used sunshine duration to assess the SSR variability in Brazil. A
47 similarity between most of these studies is the fact that they had to rely on reanalysis, modeling data
48 and indirect estimators of SSR (like sunshine duration), with the only of the abovementioned studies
49 that used ground observations being limited to a small region in Venezuela. This leaves regions such
50 as the densely populated southeastern Brazil or the highly climate-relevant Amazon region without
51 any direct assessment of the regional SSR long term variability. Yamasoe et al. (2021) presented and
52 discussed a SSR time series of fifty-six years measured in the city of Sao Paulo, and that is, to our
53 knowledge, the longest and most detailed analysis of directly observed SSR in South America. All
54 these studies provide different pieces of information about SSR variability in this part of the world,
55 however, none of them provide a large scale assessment of the long term SSR decadal trends using
56 ground observations of SSR, as done for regions like Europe (e.g. Chiacchio and Wild, 2010;
57 Pfeifroth et al., 2018), China (e.g. Yang et al., 2018) or the United States (e.g. Long et al., 2009).

58 To try to tackle this gap in literature, we made use of the availability of SSR data from
59 automated meteorological stations from the Instituto Brasileiro de Meteorologia (INMET) from 2001
60 onwards to provide a large scale assessment of SSR decadal trends and underlying causes at the
61 beginning of the 21st century in the Brazilian territory, which covers approximately half of the South
62 American continent. The objective of this study is to present the in-situ observed SSR decadal trends
63 around Brazil in the first two decades of the 21st century and discuss their underlying causes. This is
64 done at the regional level, rather than locally, by selecting stations in strategic locations around the
65 Brazilian territory and grouping them into station composites. With this study we intend to help to
66 reduce the under representativity of Global Dimming and Brightening (GDB) studies in South
67 America.

68 **2. Data and methods**

69 **2.1 In situ SSR and cloud cover measurements**

70 Surface solar radiation data for 32 of the 34 stations is collected and controlled the Instituto
71 Brasileiro de Meteorologia (INMET) and was retrieved from the BDMEP portal (available at: [https://
72 bdmep.inmet.gov.br/](https://bdmep.inmet.gov.br/) (last access 27 Oct 2023)). The stations were chosen based on data availability in
73 the regions of each composite used in this study (see section 2.4). The data was retrieved at hourly



74 time resolution. All data was tested at the hourly time scale for consistency using the physical and
75 extremely rare limits established by Long and Dutton (2002). The hourly values were further
76 converted into daily means by simply averaging the 24 hourly values in a day. If one hourly value was
77 missing (due to either lack of data or removal during quality test) the value was filled linearly using
78 the previous and next hours. If more than one hourly value was missing, the daily value was not
79 calculated. Daily values were further converted into monthly values by simply averaging the daily
80 means. Monthly values were only calculated when at least 70% of the days in a month were available.
81 Further conversion from monthly to annual values again occurred by simply averaging the 12 months.
82 If one or two monthly values went missing, the long term mean for that month would be used instead,
83 and the annual mean was still calculated. If more than two monthly values were missing, then the
84 annual value was not calculated.

85 The BSRN (Baseline Surface Radiation Network, Ohmura et al., 1998; Driemel et al., 2018)
86 station at Florianopolis was also used in this study. Its data was provided at 15-minute intervals. Data
87 from the station operated by the Instituto de Astronomia, Geofísica e Ciências Atmosféricas of the
88 Universidade de São Paulo (IAG/USP), located in the city of Sao Paulo was also used. Data from this
89 station was provided as daily means. Both time series were also checked for consistency with the
90 same procedure applied to the INMET stations, at the hourly time scale for the BSRN station and at
91 the daily time scale for the IAG/USP station. The SSR long term variability at the Sao Paulo station
92 was previously carefully analyzed by Yamasoe et al. (2021). This station also has the longest time
93 coverage among all of the stations used in this study: all the other stations only have data after 2000,
94 while this stations has available data from decades earlier. But we limited the analysis to the period
95 with coverage of the other stations because we intend to investigate the SSR variability at the regional
96 level (composites) rather than at the local level (individual station). The procedure to convert from
97 sub-daily to daily averages, from daily to monthly and from monthly to annual values at these two
98 stations was the same as the procedure used for the INMET stations.

99 Cloud cover data was also retrieved through the BDMEP portal from the INMET. The stations
100 were the same as used for the INMET SSR measurements with the addition of data from
101 Florianopolis. In Florianopolis, where the SSR data is originally from BSRN, the location of the SSR
102 and the cloud measurements differ by a few kilometers. Cloud cover data is collected from visual
103 inspections at 00, 12 and 18 UTC and is provided in units of tenths (1/10) of cloud cover.. The daily
104 cloud cover values used in this study are a result of the average from the 12 and 18 UTC observations.
105 This is equivalent to 9 and 15 local time at most of the stations used in this study (8 and 14 for the
106 westernmost stations). At the Sao Paulo station, the diurnal cloud cover values are a result of hourly
107 observations between 7 and 18 local time. Cloud cover data was converted into monthly and then
108 annual values using the same procedure as used for the SSR data. The cloud cover data is also used to
109 calculate the Cloud Cover Radiative Effect (CCRE), following the procedure described by Norris and
110 Wild (2007). This variable gives an estimation of the change in SSR produced by changes in cloud
111 cover.



112 **2.2 Satellite and reanalysis data**

113 To investigate Aerosol Optical Depth (AOD) variability, we used data from the CAMS
114 (Copernicus Atmosphere Monitoring System) reanalysis (Inness et al., 2019), provided by ECMWF.
115 This product has monthly time steps and spatial resolution of approximately 80 km, with temporal
116 coverage starting from 2003. To assess the Aerosol Absorption Optical Depth (AAOD) at 500 nm we
117 used data from the OMAERUV aerosol algorithm from the Ozone Monitoring Instrument (OMI,
118 Torres et al., 2007). The product is provided at daily time resolution and 1-degree resolution, and is
119 available from 2004 onwards. Due to the frequent occurrence of missing daily values (due to different
120 aspects, such as cloudy scenes), conversion from daily to monthly values was done only when at least
121 two days in a month were available. From monthly to annual values the conversion was only
122 performed when at least 11 of the 12 months had available data (missing month would be filled with
123 long term mean). We should also highlight that aerosol absorption is a variable highly dependent on
124 the spectral region, thus the absorption at 500 nm could not be representative for the whole spectrum.

125 We also used shortwave radiative fluxes measured at the Top of the Atmosphere (TOA) by the
126 CERES (Cloud and Earth's Radiant Energy System, Doelling et al., 2013) instruments on board of the
127 satellites Terra and Aqua. The CERES-EBAF product (Loeb et al., 2018), used in this study, provided
128 TOA shortwave fluxes at monthly time intervals and 1-degree spatial resolution, from 2000 onwards.

129 Anthropogenic emissions were assessed using EDGAR (Emissions Database for Global
130 Atmospheric Research, Crippa et al., 2018). The data provides anthropogenic emission estimates at
131 0.1 degree spatial resolution and does not consider large scale biomass burning, land use change and
132 forestry (Crippa et al., 2018). For this study we acquired the data in annual values and in units of kg
133 $m^{-1} s^{-1}$. The unit was further converted to kg $grid^{-1} year^{-1}$ (kg emitted for each 0.1 degree grid per
134 year). Finally, total column water vapour was obtained from the ERA5 reanalysis (Hersbach et al.,
135 2020), which provides data with a 0.25 degree spatial resolution and monthly time resolution. Cloud
136 cover from ERA5 was also used as supporting information in addition to the previously mentioned
137 SYNOP cloud cover, measured in-situ.

138 **2.3 Clear-sky SSR**

139 Time series of clear-sky SSR were derived using two different methods. At all stations we
140 used (1) the clear-sky method proposed by Correa et al. (2022), and at the stations with Synop cloud
141 cover data we also (2) derived clear-sky using cloud cover information. We applied both methods on
142 the daily time series. For the first method, we calculate station specific daily transmittance thresholds
143 for every month of the year. Days with transmittance lower than this threshold for the specific station
144 in the respective month are flagged as cloudy and removed. Days with transmittance above the
145 thresholds are flagged as clear-sky. As this method relies on the reduction of atmospheric
146 transmittance under cloudy conditions, its main weakness is associated with extreme aerosol events
147 that could suddenly strongly reduce transmittance. Thus this method is not well suited for the analysis
148 of high frequency (interannual) variability, but it has been shown adequate for assessment of long
149 term trends (Correa et al., 2022).



5

150 For the second method, we simply used in-situ observations of cloud cover to identify cloudy
151 scenes. We set the threshold of cloud cover to two tenths (20%), where any day with cloud cover
152 above that was flagged as cloudy and removed. The choice of the cloud cover threshold represents a
153 trade-off, where low thresholds (say, 0%) would completely avoid any cloud signal but would also
154 remove days with low cloud occurrence, where the effects of cloud-free processes still dominate, and
155 leave the time series with very few valid values. For this reason, we allowed a higher threshold,
156 assuming that on days with such low cloud cover (0-20%) the cloud-free processes still dominate the
157 signal of the SSR variability.

158 In both methods, the removal of cloudy days results in clear-sky SSR time series with many
159 gaps. Thus, special care should be taken when converting from daily to monthly values and from
160 monthly to annual values. Monthly values were only calculated when at least two daily values were
161 available for the respective month. But before taking their average, each available daily value is
162 normalized to the 15th day of the month by multiplying the daily irradiance with a normalization
163 factor. This normalization factor is a result of the ratio between the TOA daily irradiance at the 15th
164 day of the month and at the day flagged as clear-sky. This is done to correct for the solar geometry at
165 different times of the month. From monthly to annual values the procedure is the same as done for all-
166 sky SSR: the calculation is done when at least 10 months are available, with missing values being
167 replaced by long term means. When less than 10 months are available, the annual means are not
168 calculated.

169 **2.4 Fractional atmospheric column absorption**

170 The daily fractional atmospheric column absorption (F_{abs}) was calculated for every station by
171 combining SSR measured at the surface, surface albedo from ERA5 at the 0.25x0.25 degree spatial
172 resolution and incoming and outgoing shortwave radiation at TOA from CERES-SSF 1deg from the
173 Terra satellite (1x1 degree spatial resolution) and daily time resolution. These variables were
174 combined in equation 1 to calculate F_{abs} .

$$175 \quad F_{\text{abs}} = 1 - (SW_{\text{upTOA}}/SW_{\text{downTOA}}) - ((1-\text{albedo}_{\text{SFC}})*(SW_{\text{downSFC}}/SW_{\text{downTOA}})) \quad (1)$$

176 SW_{upTOA} is the outgoing shortwave radiation at TOA, SW_{downTOA} is the incoming shortwave
177 radiation at TOA, $\text{albedo}_{\text{SFC}}$ is the surface albedo and SW_{downSFC} is the SSR. Thus, the term $(SW_{\text{upTOA}}/$
178 $SW_{\text{downTOA}})$ represents the fraction (0-1) of the incoming shortwave radiation at the TOA which is
179 reflected back to space, and the term $((1-\text{albedo}_{\text{SFC}})*(SW_{\text{downSFC}}/SW_{\text{downTOA}}))$ represents the fraction
180 (0-1) of the incoming shortwave radiation at the TOA which is absorbed at the surface. Then, F_{abs}
181 represent the fraction of the incoming shortwave radiation at TOA which is absorbed within the
182 atmosphere column. F_{abs} values can range between 0 and 1, where 0 would represent no atmospheric
183 absorption and 1 would represent a black body absorption by the atmosphere.

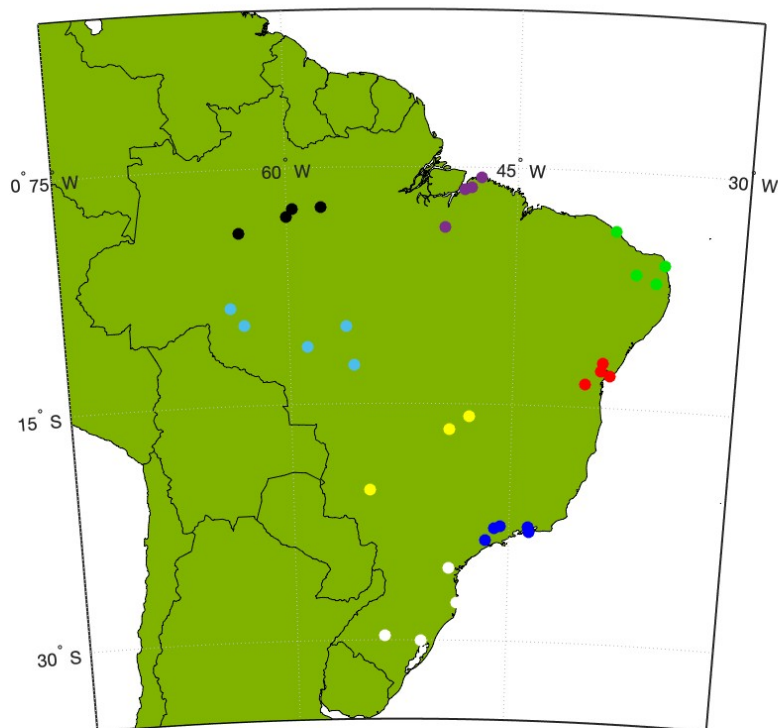
184 **2.5 Selection of station composites**

185 The stations used in this study were divided into eight composites based on geographical
186 proximity, demographics and atmospheric features found in Brazil. That is, the composites were



6

187 organized with the intent of covering different climate characteristics around the country and, when
188 possible, included data from big (> 1 million inhabitants) cities for better spatial reference. They are:
189 [1] Manaus region, [2] Belem region, [3] Fortaleza region, [4] Salvador region, [5] South Amazon, [6]
190 Midwest Brazil, [7] Southeast Brazil and [8] South Brazil. The location of all stations are shown in
191 Figure 1, and colors denote the different composites. Each composite is composed of three to five
192 stations. Based on literature review, Reboita et al. (2010) divided the precipitation regimes in South
193 America in 8 regions, out of which five regions occurred in the Brazilian territory. Ferreira and
194 Reboita (2022) revisited the topic and applied a non-hierarchical clustering technique to classify the
195 precipitation regimes in South America. The authors also found 8 different precipitation regimes in
196 the continent and only minor spatial differences to the previous study, with five of the regimes being
197 present in the Brazilian territory. All of them were at least partly represented by the composites.



198

199 **Figure 1: Map of Surface Solar Radiation stations and composites used in this study. Colors represent the**
200 **different composites: Black = Manaus region; Purple = Belem region; Green = Fortaleza region; Red =**
201 **Salvador region; Light Blue = South Amazon; Yellow = Midwest Brazil; Dark blue = Southeast Brazil;**
202 **White = South Brazil.**



203 In the north of Brazil two composites were centered around the two biggest cities in the
204 Brazilian Amazon, (1) Manaus and (2) Belem. Precipitation and cloudiness in both regions is strongly
205 tied to local to mesoscale phenomena, like local convection, sea breeze circulation and squall lines,
206 with the Intertropical Convergence Zone (ITCZ) being the most important large scale phenomena,
207 playing a major role for the seasonality of precipitation (Fisch et al., 1998). Feedbacks with the
208 Amazon rainforest are also important, especially the recycling of precipitation. But regarding biomass
209 burning in the Amazon, the most important area is located in the southern part of the Amazon (Artaxo
210 et al., 2006), south of both locations. The occurrence of the South American Low Level Jet (Vera et
211 al., 2006), important for moisture and aerosol transport from the Amazon to Southeastern Brazil,
212 leaves the locations of Belem and Manaus out of the area with the strongest influence of biomass
213 burning aerosols from the Amazon. Still, the influence of aerosols from the forests (either biogenic or
214 biomass burning related) should not be neglected, and most importantly, the importance of
215 anthropogenic emissions from such big population centers should be taken into account.

216 In the northeast of Brazil, the composites of (3) Fortaleza and (4) Salvador share similar
217 general characteristics regarding precipitation and cloudiness regimes. The stations in these
218 composites are also centered around big population centers (Fortaleza and Salvador), where
219 anthropogenic emissions should be taken into account. The biggest difference to the composites
220 around Manaus and Belem, is that these two composites are not located in the Amazon region. But
221 they are located in the same precipitation regime division proposed by by Ferreira and Reboita (2022),
222 with two stations of the Fortaleza composite being located in a different subdivision.

223 The composite (5), South Amazon, was chosen to cover the region under the strongest
224 influence of biomass burning aerosols from the Amazon (Artaxo et al., 2006). The stations in this
225 composite are located in a different subdivision by Ferreira and Reboita (2022), where large scale
226 phenomena (such as the Bolivian high, the South Atlantic Convergence Zone and cold fronts) play an
227 important role for the cloud formation. This composite is not centered around a big city, and the most
228 populated city in the area is Porto Velho, with a population of approximately 500'000 people (IBGE,
229 2022). A few degrees south of the South Amazon composite, are the stations of the (6) Middle West
230 Brazil composite. They are located approximately halfway between the South Amazon composite and
231 the densely populated Southeast Brazil. It is a dry region mostly influenced by large scale phenomena,
232 compared to the north and northeast regions of Brazil. The biggest city in the composite is Brasilia.

233 The Southeast is the most densely populated area in Brazil, where big centers like Sao Paulo
234 and Rio de Janeiro are located. Like the Middle West and South Amazon composites, cloud formation
235 in this region is mostly associated with large scale phenomena (Reboita et al., 2010; Ferreira and
236 Reboita, 2022). The (7) Southeast Brazil composite covers this area. The transport of humidity and
237 aerosols from the south Amazon are both relevant aspects to consider. But regarding aerosols,
238 anthropogenic emissions from the large population centers should be more relevant. The last station
239 composite covers the Southernmost part of the country. The (8) South Brazil composite is entirely
240 located in subtropical latitudes, and covers its own precipitation regime subdivision from Ferreira and
241 Reboita (2022). Large scale phenomena like fronts and subtropical cyclones play a major role for



8

242 cloud formation and moisture transport from the ocean. It is also a densely populated region, with big
243 cities like Porto Alegre, Curitiba and Florianopolis, thus, anthropogenic aerosol emissions should be
244 taken into account.

245 The whole discussion in this study revolves around these eight composites. Each variable was
246 fully processed and converted to annual values at the station level, and only after that, they were
247 grouped with the other stations in the respective composite. The list of stations in each composite can
248 be found in Table A1 (in appendix).

249 **2.6 Trend calculations**

250 Decadal trends of SSR and most other variables presented in this study were calculated using
251 a Linear Least Squares (LLS) regression, with the confidence intervals being calculated using
252 equation 4 from Nishizawa and Yoden (2005). Cloud cover time series, in most cases, did not have the
253 residuals normally distributed, thus, to account for that, we calculated their trends using the Sen's
254 slope (Sen, 1968) and Mann-Kendall test (Mann, 1945; Kendall, 1975). Trends of ground
255 observations were calculated for the whole time availability of the composites, however, as the time
256 availability varies from one composite to the other, the periods used for trend calculations vary by a
257 few years. SSR trends are displayed in units of W/m^2 per decade. The period considered in each
258 composite is displayed in Table 1.

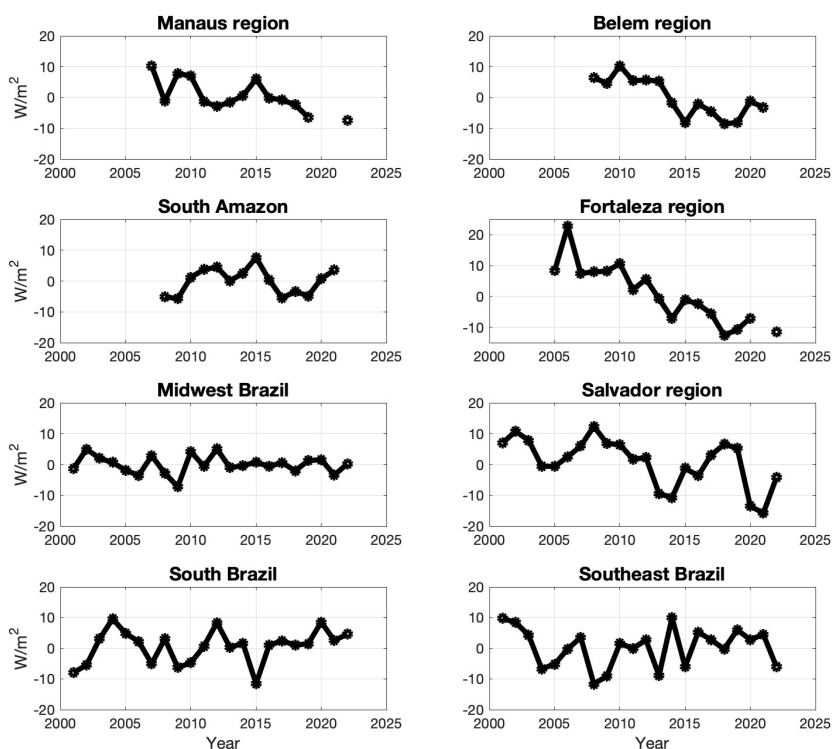
259 **3. Results**

260 **3.1 All-sky and clear-sky SSR trends**

261 Figure 2 shows the all-sky SSR time series of the 8 composites analyzed in this study. All
262 trends calculated in this study are shown in Table 1.



9



263

264

265

266

Figure 2: Time series of all-sky Surface Solar Radiation annual anomalies from the eight composites used in this study. Each composite is composed of three to five stations. Anomalies in reference to the composites entire period (shown in table 1).

267

Composites	Period	All-sky	Clear-sky (Correa et al., 2022)	Clear-sky (Synop)*	Synop Cloud cover	All-sky atm abs	Clear-sky atm abs	CCRE
Manaus region	2007-2022	-8.8 ± 4.2	-2.0 ± 2.3	-	1.2 [0.0; 2.0]	0.0205 ± 0.007	0.0048 ± 0.0074	-1.1
Belem region	2008-2021	-11.7 ± 5.8	-4.8 ± 2.5	-	1.4 [0.4; 1.3]	0.0160 ± 0.0096	-0.0002 ± 0.0056	-1.5
Fortaleza region	2005-2022	-16.0 ± 4.2	-2.7 ± 1.8	-	0.8 [-1.3; 2.5]	0.0340 ± 0.012	0.0030 ± 0.0113	-0.4
Salvador region	2001-2022	-7.0 ± 4.5	-3.7 ± 1.7	-	1.9 [0.7; 3.1]	0.0163 ± 0.0078	0.0098 ± 0.0057	-1.3
South Amazon	2008-2021	0.8 ± 6.4	1.6 ± 1.8	-	-	0.0054 ± 0.0154	-0.0032 ± 0.0074	-
Midwest Brazil	2001-2022	-0.4 ± 2.1	-1.8 ± 1.1	-2.5 ± 1.9	-1.3 [-2.1; -0.3]	0.0050 ± 0.0032	0.0051 ± 0.0050	1.4



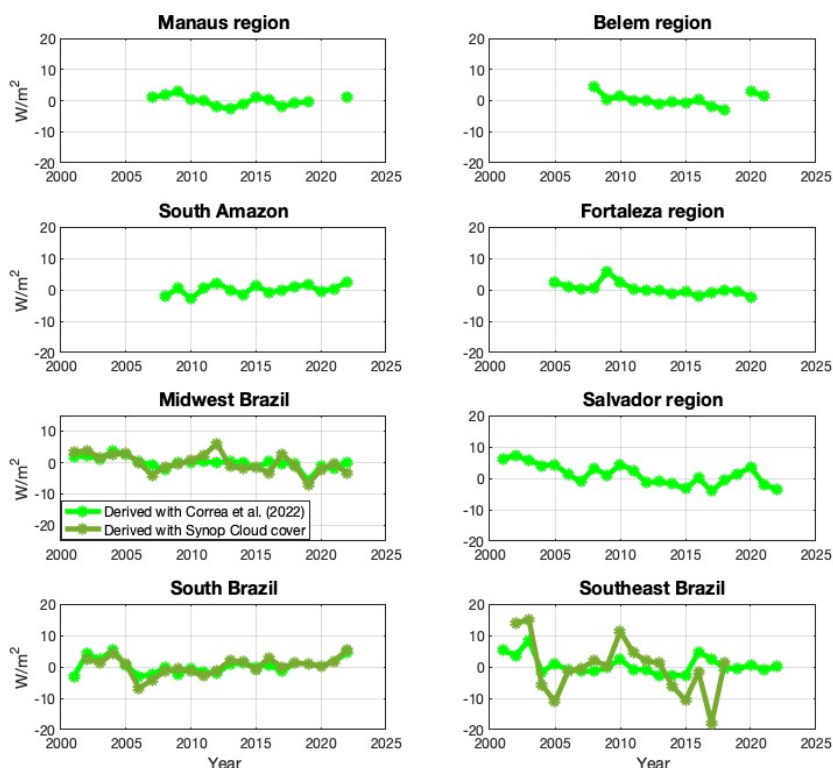
268

Southeast Brazil	2001-2022	-0.1 ± 4.5	-1.6 ± 1.9	-7.7 ± 8.5	-3.7 [-5.5; -1.3]	0.0016 ± 0.0059	0.0059 ± 0.0072	3.9
South Brazil	2001-2022	2.0 ± 3.8	1.1 ± 4.1	1.2 ± 1.9	-0.2 [-1.3; 0.7]	0.0002 ± 0.0053	-0.0027 ± 0.0074	0.2

269 **Table 1 - Trends (in W/m² per decade) for all-sky and clear-sky (using Correa et al., 2022, and using**
 270 **Synop cloud cover) SSR, all-sky and clear-sky (using Correa et al., 2022) fractional atmospheric**
 271 **absorption and Synop cloud cover at the 8 composites used in this study. Cloud Cover Radiative Effect**
 272 **(CCRE) referring to the Synop cloud cover trend also included. SSR trends in W/m² per decade;**
 273 **fractional atmospheric absorption trends in fraction (values between 0 and 1) per decade; Synop cloud**
 274 **cover in % per decade; and CCRE in W/m². Trends in bold are statistically significant at the 95%**
 275 **confidence level. Stations in each composite are listed in Table A1 (in appendix).**

276 ***Missing values for clear-sky Synop trends occur due to the limited amount of Synop cloud cover data (0**
 277 **stations for the South Amazon composite, 2 out of 4 stations for Belem and Manaus composites) or due to**
 278 **not enough days flagged as clear-sky in order to generate a clear-sky time series (according to the**
 279 **procedure described in section 2.3).**

280 In the North and Northeast Brazil composites (Belem, Manaus, Fortaleza and Salvador
 281 composites) statistically significant (at the 95% confidence level) negative SSR trends (dimming)
 282 were observed. In the Southeast and Middle West composites, trends were negative, although near
 283 zero and statistically insignificant. Southern Amazon and South Brazil composites both show
 284 statistically insignificant positive SSR trends (brightening). This reveals a contrasting spatial
 285 distribution of the all-sky SSR trends in the first two decades of the 21th century in Brazil: while
 286 strong dimming occurred in the northern half of the Amazon region and in the northeastern coastal
 287 region, near-zero to weak positive SSR trends occurred from the southern part of the Amazon down to
 288 the south of Brazil, including the central area of the country and the densely populated southeastern
 289 region. Figure 3 shows the time series of clear-sky SSR derived with the two methods used in the
 290 study.



291

292 **Figure 3: Time series of clear-sky Surface Solar Radiation annual anomalies (in reference to the**
 293 **composite full time coverage, shown in Table 1) from the eight composites used in this study. Light green**
 294 **time series derived using the method by Correa et al. (2022) and olive green time series derived using**
 295 **Synop cloud cover.**

296 Time series of clear-sky SSR could not be derived in five out of the eight composites (see
 297 figure 3 and table 1). In the South Amazon composite no station had Synop cloud cover available. For
 298 Belem and Manaus regions composites only two out of the four stations in each composite had Synop
 299 cloud cover data available and this limited the amount of data available to derive clear-sky for the
 300 composite. For both Fortaleza and Salvador region composites, Synop cloud cover data was available
 301 for all stations, however, the few occurrences of low cloud cover days did not enable the
 302 derivation of clear-sky SSR time series following the procedure described in section 2.3.

303 Clear-sky SSR time series show in general a similar pattern as observed in all-sky. All of the
 304 composites show the same sign as the trends in all-sky, and six of them also indicate the same
 305 statistical significance (or insignificance). The only exceptions are the Middle West and Manaus
 306 composites. The former showed statistically insignificant negative trends in all-sky SSR, but
 307 statistically significant negative clear-sky SSR trends. The opposite occurred in the Manaus



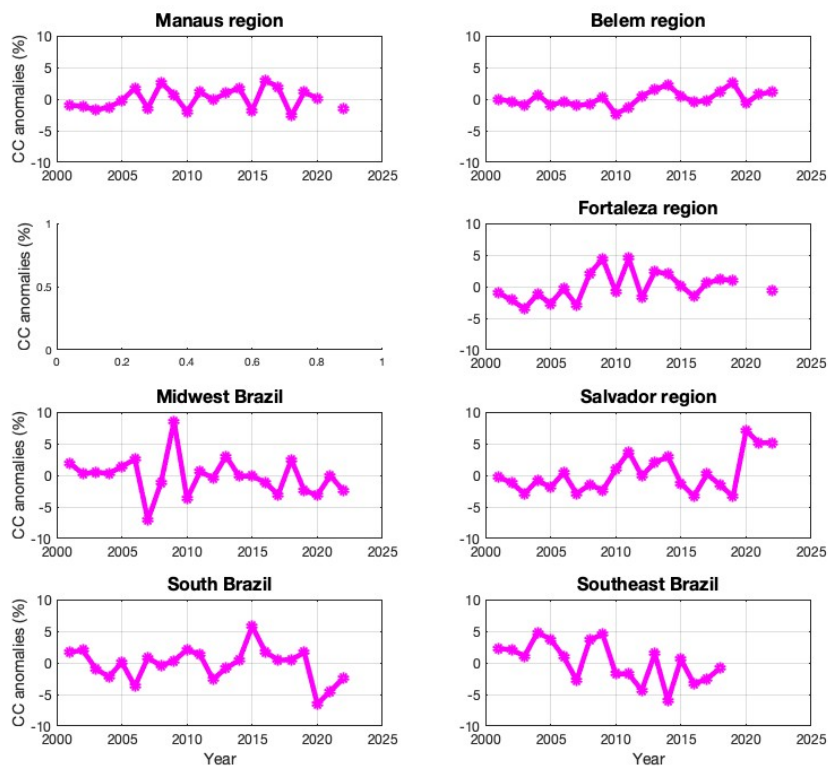
12

308 composite: statistically significant all-sky SSR trends and statistically insignificant clear-sky SSR
309 trends. These results were found by both clear-sky methods used in the study, although with slightly
310 different values in the trends. Regarding the magnitudes of the clear-sky SSR trends in comparison to
311 the all-sky trends, another general pattern could be observed. In all composites with statistically
312 significant negative all-sky SSR trends (Belem, Manaus, Fortaleza and Salvador), the clear-sky SSR
313 trends showed a substantially smaller magnitude. In the Southeast and Middle West, both with near-
314 zero all-sky SSR trends, the clear-sky SSR trends were both negative and of larger magnitude than
315 their all-sky counterparts. In the two composites with observed statistically insignificant all-sky SSR
316 brightening (South Amazon and South Brazil), the clear-sky SSR trends showed similar magnitudes
317 as the all-sky SSR trends.

318 These results indicate that the clear-sky processes in the atmosphere contributed to the
319 observed all-sky SSR trends in the whole of Brazil, but only in the Southern Amazon and in South
320 Brazil their magnitude might have been large enough to be able to explain the observed SSR trends.
321 Further analysis is thus needed to enlighten other relevant contributors to the decadal SSR trends in
322 Brazil.

323 **3.2 Cloud cover, AOD and water vapour trends**

324 Figure 4 shows the SYNOP cloud cover time series for 7 of the 8 composites analyzed in the
325 study (the cloud cover time series for the Southern Amazon composite could not be constructed due to
326 too much missing data). The associated trends can be found in Table 1.



327

328 **Figure 4 - Time series of annual mean Synop cloud cover for seven of the eight composites used**
329 **in this study. Not enough data was available to derive a time series for the South Amazon**
330 **composite.**

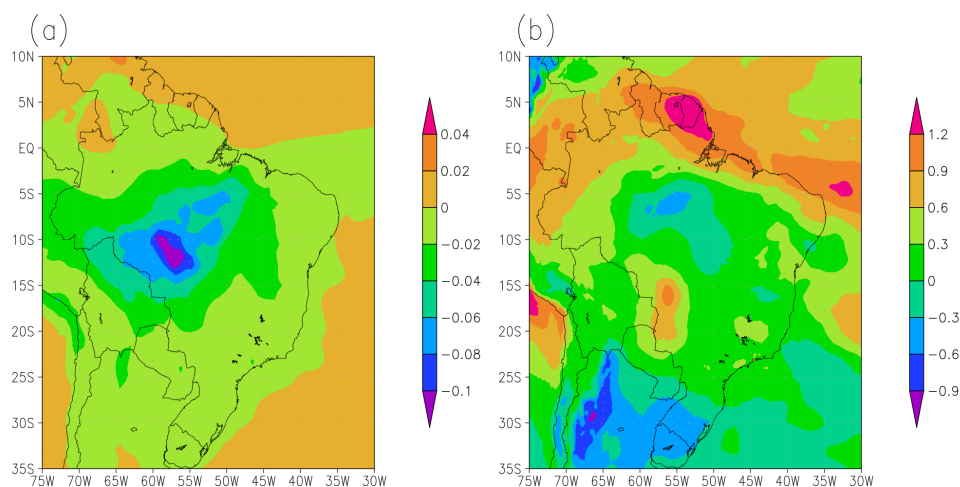
331 Cloud cover trends are in most cases consistent in sign with the all-sky SSR trends. That is,
332 positive (negative) trends in cloud cover occurring during a period of negative (positive) SSR trends.
333 That is the case for the four composites with statistically significant all-sky SSR dimming (Belem,
334 Manaus, Fortaleza and Salvador). They all show positive trends in cloud cover, and all, except
335 Fortaleza, show statistical significance. This is consistent in the sense that the increase in cloud cover
336 contributes to the observed decrease in SSR, especially considering that the magnitude of the clear-
337 sky SSR trends at these locations was significantly smaller than the all-sky SSR trends. However,
338 quantitatively, the small magnitude of the cloud cover trends (between 0.8 and 1.9 % per decade)
339 challenges any hypothesis of a major contribution of cloud cover changes to the decadal SSR trends.
340 That is, the cloud cover trends are too small and the estimated CCRE (table 1) suggests only a minor
341 contribution from cloudiness to the SSR trends.

342 Cloud cover trends show near-zero values in the South region, suggesting no major cloud
343 contribution to the SSR trends. Southeast and Middle West show both statistically significant negative
344 trends in cloud cover, with remarkably strong values in SE (-3.7 [-5.5; -1.3] % per decade). Both
345 composites show near-zero but negative all-sky SSR trends, with stronger negative clear-sky SSR



346 trends. Thus, the cloud cover trends exert an opposite effect to the one of the clear-sky processes at
347 both composites. This is also consistent, in the sense that with clear-sky processes and cloud cover
348 having competing opposite effects, if their magnitude is similar, their effects cancel out, and the
349 resulting all-sky SSR trend would be near zero.

350 Figure 5 shows the decadal trend maps of annual AOD in the 2003-2020 period from CAMS
351 reanalysis and of total column water vapour in the 2001-2020 period from ERA5.



352

353 **Figure 5 - Maps of decadal trends of (a) AOD [unitless] in the 2003-2020* period from CAMS**
354 **reanalysis and of (b) total column water vapour [in kg m⁻²] in the 2001-2020 period from ERA5.**
355 ***The dataset was available only from 2003 onwards.**

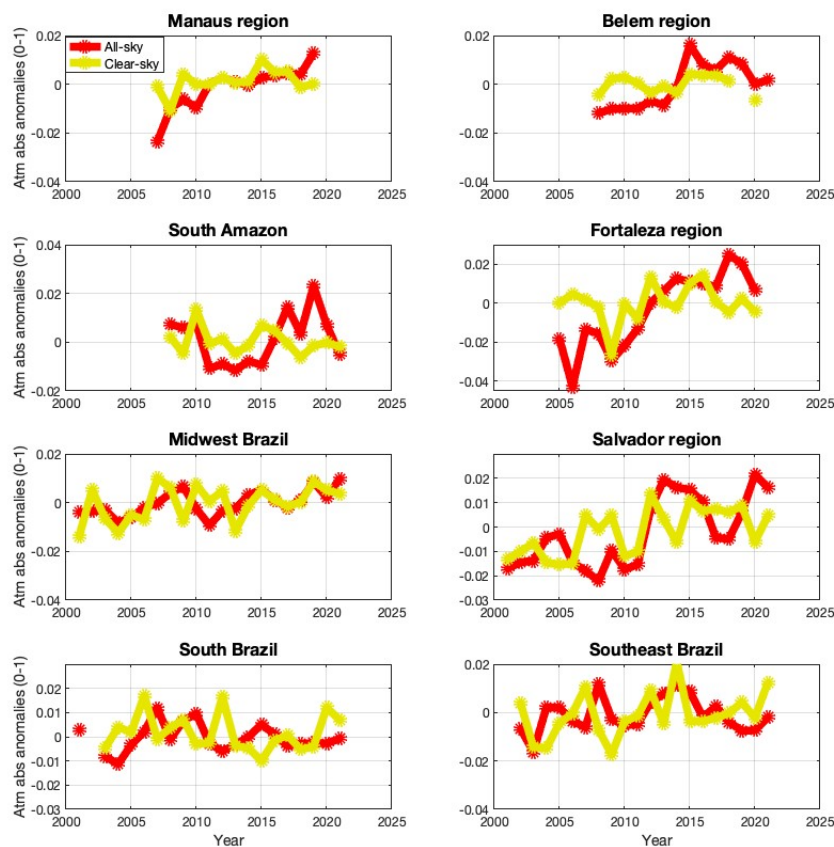
356 In Figure 5 (a) we see a strong negative AOD trend in the Southern Amazon in the period, and
357 slightly negative to near-zero trends in the rest of the country. The process that dominates the AOD
358 trends in the Southern Amazon (and in the whole country) is the reduction of biomass burning in the
359 Amazon region. The Southern part of the Amazon region is the area that suffers most from the
360 biomass burning (Artaxo et al., 2006), especially in the dry season during the southern hemisphere
361 summer. A reduction in forest fires at the beginning of the 21st century has been reported (Silva Junior
362 et al., 2021), and its effect is clear in the AOD trends. This result is consistent with the observed clear-
363 sky SSR brightening in the Southern Amazon, but challenges the negative clear-sky SSR trends
364 observed in most of the country. This suggests that changes in AOD were not primarily responsible
365 for the clear-sky SSR trends in the whole of Brazil, with the exception of the Southern Amazon
366 region.



367 The water vapour trend map (Figure 5 (b)) shows remarkably negative trends in the central
368 Amazon, in a region around the east coast of Brazil and in the southernmost part of the country.
369 Remarkably positive trends are present from the middle Western Brazil (south of the Amazon region)
370 stretching to Southeastern Brazil, and in the northeast and north coastal regions of the country. The
371 spatial distribution of the decadal variability of water vapour does not generally fit to the observed
372 clear-sky SSR trends. We used these trends to estimate the change in atmospheric clear-sky absorption
373 due to solely water vapour, using the empirical model presented by Hakuba et al. (2016). Based on
374 these estimations, even in a region with strong water vapour trend such as Midwest Brazil, these
375 changes would be responsible for an increase in atmospheric clear-sky absorption (and consequently
376 decrease in SSR) of approximately 0.4 W/m^2 per decade. This is almost one order of magnitude
377 smaller than the clear-sky SSR trends in the region (-1.8 and -2.5 W/m^2 per decade, for clear-sky
378 conditions based on Correa et al. (2022) and Synop cloud cover, respectively). This suggests that the
379 water vapour contribution to the observed clear-sky SSR trends, when existed, was only minor.

380 **3.3 Atmospheric absorption and Anthropogenic emissions**

381 To better understand the reasons behind the observed clear-sky SSR trends and the overall
382 processes responsible for the all-sky SSR trends, we analyzed the changes in fractional atmospheric
383 absorption under all-sky and clear-sky conditions. Figure 6 shows these time series for the composites
384 considered in this study both under all-sky and clear-sky conditions.



385

386

387

Figure 6: Time series of all-sky (red) and clear-sky (green) fractional atmospheric column absorption annual anomalies for the eight composites used in this study.

388

389

390

391

392

393

394

395

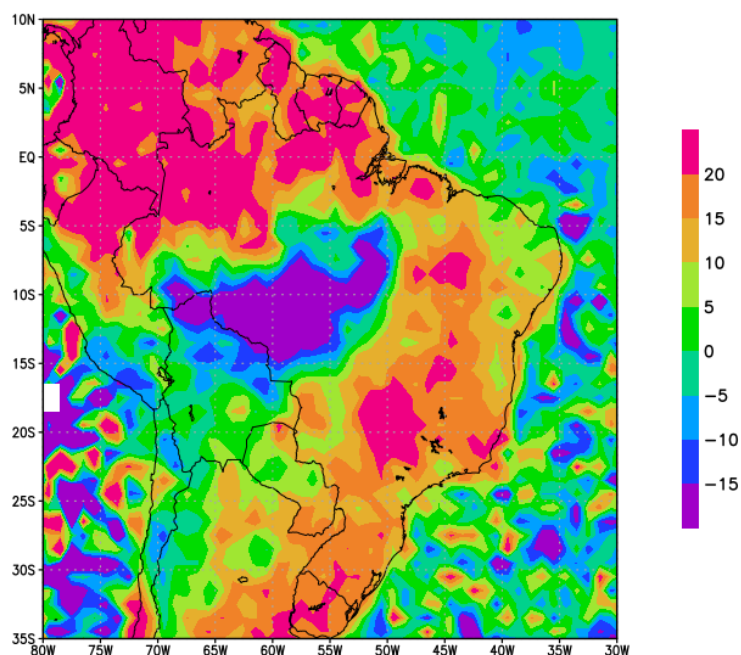
396

397

The fractional atmospheric absorption under all-sky conditions increased in most of the composites in the first two decades of the 21st century. Five composites showed statistically significant positive trends in FAB_{as} , they are: Manaus, Belem, Fortaleza, Salvador and Middle West. The other composites also showed positive trends, but they were statistically insignificant. Under clear-sky conditions, the trends are obviously smaller, as the cloud induced multiple scattering does not play a role in enhancing column absorption. Only in the Salvador and Middle West composites statistically significant positive trends were observed in the atmospheric absorption under clear-sky conditions. All the other composites show statistically insignificant trends with the same sign as their all-sky counterparts, with the exception of the South Amazon, which shows negative trends under clear-sky, contrasting to a positive trend under all-sky conditions.



398 These results reveal two important aspects of the SSR variability in Brazil. First, in seven out
399 of the eight composites the changes in clear-sky absorption fit to the clear-sky SSR trends. That is,
400 increasing (decreasing) clear-sky atmospheric absorption was always linked to a decrease (increase)
401 in clear-sky SSR. Secondly, the presence of clouds greatly increased atmospheric absorption (not
402 shown) but also its trends. This has most likely happened because of the intensification of multiple
403 scattering occurring under partially cloudy skies, resulting in a magnification of the effects seen in
404 clear-sky conditions. This is reinforced by the fact that the strongest all-sky atmospheric absorption
405 trends were found in the four cloudier composites (Manaus, Belem, Fortaleza and Salvador), which
406 happen to be the four composites with statistically significant negative all-sky SSR trends (dimming).
407 Even though these results fit to each other, they also suggest that AOD only showed strong trends in
408 the South Amazon region, and that water vapour only contributed as a minor part to the observed
409 changes in atmospheric absorption (see discussion above). Thus, this raises the question of what could
410 be the main responsible for the changes in atmospheric absorption in Brazil. To try to answer this
411 question, we analyzed the decadal trend in aerosol absorption optical depth (AAOD) at 500 nm from
412 OMI. The trend map is displayed in Figure 7.



413

414 **Figure 7: Relative (%) decadal trends in Absorption Aerosol Optical Depth (AAOD) in the 2005-2022**
415 **period from OMI.**

416

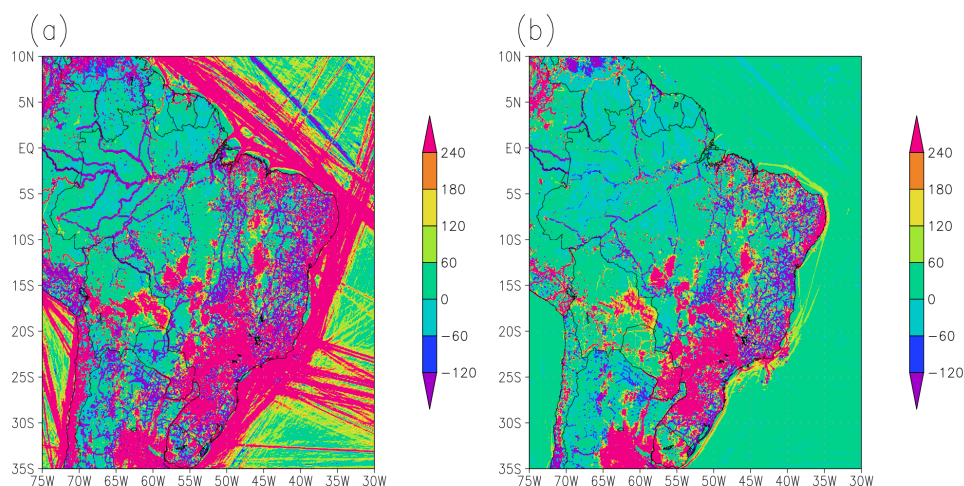
417

The map shows a clear distinction between the region under strong influence of the forest fires in the Amazon (South Amazon) and the rest of Brazil. In the South Amazon, the data shows a



18

418 decrease in AAOD in the 2005-2022 period, while in the rest of the country an increase in absorption
 419 AAOD at 500 nm is observed. The spatial distribution of the trends suggests that the reduction in
 420 AAOD in the South Amazon could be associated with the forest fires reduction also visible in the
 421 AOD trends. In the whole rest of the country, positive trends in AAOD are observed. This reveals a
 422 significant change in the optical properties of the aerosols present in Brazil in the first two decades of
 423 the 21st century, with a trend towards more absorbing aerosols (at 500 nm) in most of the country.
 424 The AOD trend map (Figure 5a) shows that in the same areas where AAOD increases, AOD remains
 425 nearly constant, with trends close to zero. In order to better visualize potential reasons for an increase
 426 in AAOD at 500 nm in most of Brazil, we also verified trends in anthropogenic SO₂ and Black
 427 Carbon emissions in Brazil. They are displayed in Figure 8.



428

429 **Figure 8: Decadal trends of annual mean (a) SO₂ and (b) Black Carbon anthropogenic emissions (in kg**
 430 **per 0.1x0.1 degree grid per decade) for the 2001-2018 period from EDGAR.**

431 They show a general increase in anthropogenic emissions in most of Brazil, especially in
 432 highly populated areas. The only areas not showing increase in anthropogenic emissions are in the
 433 Amazon rainforest. This might be counterintuitive when comparing the emissions trends (figure 8)
 434 with AOD trends (figure 5a), as the strongest AOD trend is observed in the south of the Amazon
 435 region. However, EDGAR emission estimates do not consider large scale biomass burning, land use
 436 change and forestry (Crippa et al., 2018). As discussed in section 3.2, the AOD negative trend is
 437 mostly associated with reductions in biomass burning in the first two decades of the 21st century in



19

438 the Amazon. Therefore, the biggest cause of the AOD trend (Figure 5a) is not considered in the
439 emission data used in Figure 8.

440 Even though, according to figure 8, anthropogenic emissions did not increase significantly in
441 the Amazon region, emissions still increased around the biggest cities in the region, like Manaus and
442 Belem. This is of special relevance for this study, since seven of the eight composites are centered
443 around cities with over a million inhabitants, where the large and usually increasing population (Lobo
444 and Cunha, 2019) plays an important role to the atmospheric composition. The only composite that
445 does not follow this rule is the South Amazon composite, where the biggest city is Porto Velho, which
446 in 2020 had a population of less than 500'000 people (IBGE 2022). As anthropogenically emitted
447 aerosols tend to account for a larger fraction of solar radiation absorption than natural aerosols (Wang
448 et al., 2009), this increase in anthropogenic emissions (especially of black carbon) fits to the
449 increasing AAOD in most of Brazil. Even though sulphate aerosols absorb much less shortwave
450 radiation than black carbon, the increasing presence of scattering aerosols can also have a similar
451 effect to the presence of broken clouds for atmospheric absorption (as discussed for the composites in
452 North and Northeast Brazil): they increase multiple scattering, increasing the optical path of the
453 photons, which increases the chances for absorption by the atmosphere. Therefore, the increasing
454 anthropogenic emissions fit to the observed increase in atmospheric absorption in most of Brazil in
455 the period of study. Similar results indicating a stronger impact of the changes in optical properties of
456 the aerosols than the changes in aerosol optical depth on the observed SSR trends were also found for
457 Japan in the 1990s by Kudo et al. (2012).

458 4. Discussion

459 4.1 Physical consistency of the results

460 The results of this study point to a relevant impact of changes in atmospheric absorption in at
461 least half of the regions analyzed. However, this is based on the fractional atmospheric absorption
462 data, which is derived (as described in section 2.4) by combining in situ SSR (point) measurements
463 with gridded data of surface albedo and outgoing shortwave radiation at TOA, at 0.25 and 1.0 degree
464 spatial resolution, respectively. So the first question to be addressed is whether these results can be
465 trusted even with the use of different spatial resolutions. Schwarz et al. (2018) investigated the spatial
466 representativeness of SSR measurements in many stations around the world, including four stations in
467 Brazil: Florianopolis, São Martinho da Serra (both in South Brazil), Brasilia (in Middle West) and
468 Petrolina (~ 450 km away from Salvador). The authors found a good representativity of SSR for the
469 1-degree surroundings at most stations around the world at the monthly time scales, with estimated
470 decorrelation lengths always higher than 3 degrees in all of the four Brazilian locations. Madhavan et
471 al. (2017) investigated spatial representativeness of SSR measurements at shorter time scales, and
472 found that point measurements were representative to a 10 x 10 km area in time scales up to around
473 one hour (from 26 minutes at overcast conditions to 70 minutes at broken clouds conditions). The
474 authors demonstrated that the decorrelation lengths (the distance until where the point measurement is



475 representative) increase linearly (on a log-log scale) with decreasing frequency (longer time time
476 averaging). Following the results of the study by Madhavan et al. (2017), this would lead to
477 decorrelation lengths around the order of 100 km (~1 degree) at the daily (24-hour) time scales.
478 Therefore, based on the interpretation of these results, we can expect a satisfactory consistency in the
479 results from combining point measurements at the surface with 1-degree measurements at the TOA at
480 daily time scales, as done in this study. An in-depth analysis to estimate the decorrelation lengths at
481 daily time scales of each station goes beyond the scope of the study.

482 Also regarding atmospheric absorption, previous studies (e.g. Li et al., 1995; Byrne et al.,
483 1996) have shown an enhancement in atmospheric absorption under cloudy conditions. According to
484 previous literature, such an enhancement would not be caused by cloud absorption, but by cloud
485 scattering, which increases the optical path of a photon in the atmosphere, consequently increasing the
486 chances of this photon to be absorbed by other components of the atmosphere, such as water vapour
487 and aerosols. Even though the existence of this mechanism is clear, the quantitative influence this
488 could have on the energy budget at any location would also depend on the characteristics of cloud
489 occurrence (e.g. the frequency of cloud free, overcast and partially cloudy conditions). As much as
490 cloud free conditions are not optimal for atmospheric absorption, completely overcast conditions are
491 not either. Under fully cloudy conditions, the backscattering of incoming shortwave radiation is high,
492 usually not increasing the optical path of the photons and not allowing them to reach lower levels of
493 the atmosphere, where water vapour and aerosol concentrations are higher. Thus, the high occurrence
494 of partially cloudy conditions would optimise the cloud effects on atmospheric absorption. Under
495 such conditions scattering by clouds can increase the optical path of the photons, while still allowing a
496 significant fraction of them to reach the lowest levels in the atmosphere, where water vapour and
497 aerosol concentrations are the highest. Such conditions are found in Belem, Manaus, Fortaleza and
498 Salvador, due to the importance of local convection for cloud formation in such hot and humid
499 locations. The differences in the fractional atmospheric absorption trends between clear-sky and all-
500 sky conditions at these locations reinforces this: trends under all-sky conditions are one order of
501 magnitude larger than their clear-sky counterparts. This is not observed at all the other locations,
502 which are much more dependent on mesoscale and synoptic scale cloud formation. In fact, a
503 difference in the precipitation regimes between the region where all the four above-mentioned
504 composites are located and the rest of Brazil has already been pointed out by Reboita et al. (2010) and
505 by Ferreira and Reboita (2022).

506 Chtirkova et al. (2023) investigated the potential effect of internal variability on the SSR
507 trends, and the relevance especially of Atlantic oceanic modes like the Atlantic Meridional Mode
508 (AMM) or the Atlantic Multidecadal Oscillation (AMO) to affect SSR trends by changing cloudiness
509 in Brazil. The AMM and AMO went to lower values during the period of study (2001-2022), which
510 should lead to decreasing SSR in Northeastern Brazil. This fits to the negative SSR trends in the
511 region. But it is important to note that this reduction in the oceanic modes values did not represent a
512 major phase transitions of these modes. A major increase in AMO occurred in the 1990s, and the
513 cloud cover trends (from ERA5) for the 1990-2006 period show a strong decrease in cloud cover in



514 most of Brazil, especially the south and western part of the country. No SSR data was available for
515 further investigation in this study, but the importance of internal variability for SSR trends should not
516 be neglected in future studies

517 The trends in SSR and supporting information in the eight composites made it possible to
518 separate the discussion of the causes for the SSR trends into three groups. The first group is composed
519 of the four composites in the north and northeast Brazil (Manaus, Belem, Fortaleza and Salvador).
520 Five characteristics were observed in all of these locations: 1. strong all-sky SSR dimming; 2.
521 distinguished clear-sky dimming with lower magnitude than the all-sky; 3. Positive cloud cover
522 trends; 4. Positive trends in all-sky atmospheric absorption; and 5. positive trends in clear-sky
523 atmospheric absorption but one order of magnitude smaller than their all-sky counterparts. The second
524 group is composed of the Southeast Brazil and Middle West Brazil composites. Both of these
525 composites showed: 1. Strong negative cloud cover trends; 2. negative clear-sky SSR trends; and 3.
526 negative and statistically insignificant SSR trends. The third group, composed by the South Amazon
527 and South Brazil composites show: 1. Statistically insignificant all-sky brightening; and 2. statistically
528 insignificant clear-sky brightening. Based on this, we separated the discussion on the causes for SSR
529 trends in three sections, each discussing one of the three groups.

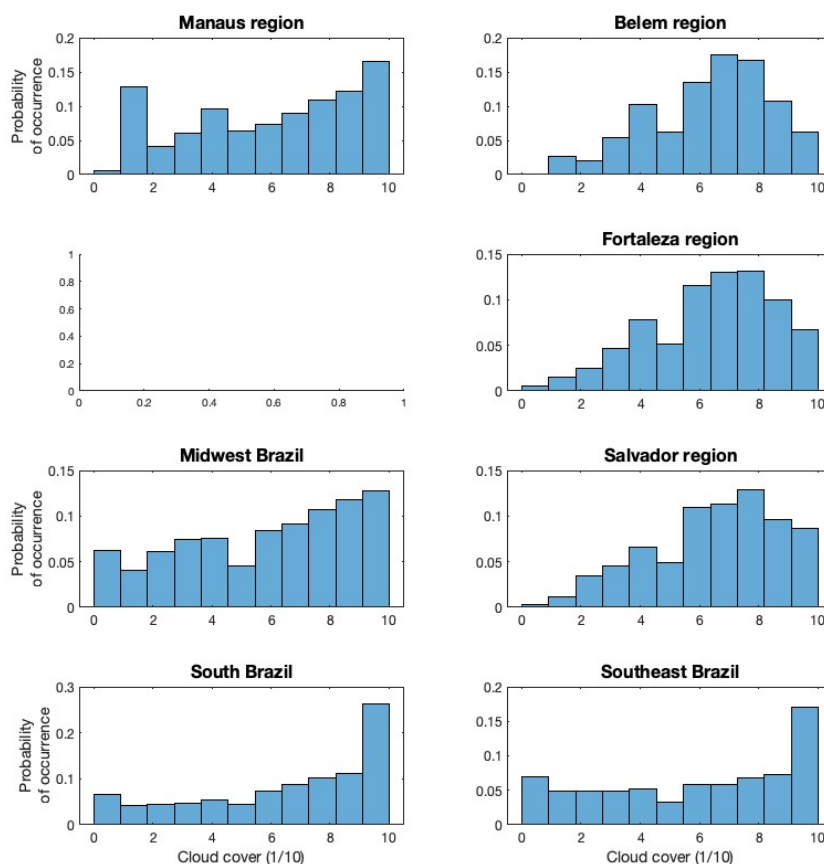
530 **4.2 Dimming in North and Northeastern Brazil**

531 In this section, we discuss the dimming observed in the Manaus, Belem, Fortaleza and
532 Salvador composites, located in North and Northeastern Brazil. All of the composites showed
533 statistically significant all-sky dimming in the period, associated with a clear-sky dimming which was
534 statistically significant in all composites, except Manaus. The difference in the magnitude of the all-
535 sky SSR trends (from -6.3 W/m^2 per decade in Salvador to -18.8 W/m^2 per decade in Fortaleza) to the
536 clear-sky SSR trends (from -2.0 W/m^2 per decade in Manaus to -4.8 W/m^2 per decade in Belem) in
537 the four composites suggests that the clear-sky processes alone are unlikely to be strong enough to
538 explain the SSR trends in these locations. However, the fact that the clear-sky trends show the same
539 sign as the all-sky trends, with (in most cases) statistical significance, indicates that processes visible
540 under clear-skies did contribute significantly to the overall trends. The contrast between all-sky and
541 clear-sky also indicates a potential contribution of changes in cloud cover to the trends. In fact, we
542 identified positive cloud cover trends, consistent with the observed reduction in SSR, but the
543 magnitude of the trends (from 0.8% per decade in Fortaleza to 1.9% per decade in Salvador) and the
544 resulting impact of these cloud cover trends on the SSR trends, estimated by the CCRE (see Table 1),
545 is small when compared to the SSR trends. Thus, our results (summarised in the table 1) suggest
546 contributions from both clear-sky processes and cloud cover to the SSR trends, but none of them show
547 a remarkable dominance compared to the other.

548 Further analysis of the atmospheric absorption showed strong positive (and statistically
549 significant) trends in atmospheric absorption in all four composites. We also found that the
550 atmospheric absorption trends were greatly enhanced by the presence of clouds. This happens because
551 the scattering by clouds increases the optical path of the photons. This effect is especially remarkable



552 under broken clouds conditions, when three-dimensional multiple scattering magnifies this effect.
553 Our findings fit to results presented by Byrne et al. (1996) and references therein, which highlight the
554 enhancement of atmospheric absorption of solar radiation under broken clouds conditions. Results
555 from Li et al. (1995) also suggested that this effect is stronger in tropical regions, and the authors
556 discuss that this is associated primarily aerosol and water vapour absorption rather than cloud
557 absorption. The characteristics of the distribution of cloudiness in the four composites, displayed in
558 Figure 9, might also play a role in this process. Stations from these composites tend to have frequent
559 occurrences of partially cloudy conditions. In the Belem, Fortaleza and Salvador composites the daily
560 cloud cover is between 25% and 80% in around two thirds of the days. For the Manaus and Midwest
561 Brazil composites this range of cloud cover occurred in around half of the days and for South and
562 Southeast Brazil composites this value is around one third. Thus, at the daily scale we see a
563 dominance of partially cloudy occurrences at three out of the four composites discussed in this
564 section. Even though the same distinguishable characteristic was not found for the Manaus composite
565 at the daily scale, based on the regionalization of precipitation regimes by Reboita et al. (2010), we
566 would expect the same finding at a more refined time scale also for the Manaus composite. That
567 would be the expectation because of the higher relevance of local convection at hot and humid
568 locations (convective clouds cause more broken cloud fields than large scale synoptic clouds) as the
569 four composites discussed in this section, in comparison to the other composites, where mesoscale
570 and synoptic meteorological systems tend to play a more important role for cloud formation. This
571 higher occurrence of broken clouds in the regions of the four composites discussed in this section then
572 tends to play an important role for the enhancement of atmospheric absorption.



573

574

575

Figure 9: Distribution of daily Synop cloud cover occurrences in seven out of the eight composites used in this study. Not enough data was available to derive a distribution for the South Amazon composite.

576

577

578

579

580

581

582

583

584

585

586

587

588

A simple multiplication between the incoming TOA radiation at each composite and the trends in fractional all-sky atmospheric absorption (shown in Table 1) reveals an estimated increase in all-sky atmospheric absorption from approximately $6 \pm 3 \text{ W/m}^2$ per decade in Belem up to $14 \pm 5 \text{ W/m}^2$ per decade in Fortaleza. If we assume that such an increase in atmospheric absorption is directly reflected in a reduction in SSR, we find that the effect of changes in atmospheric absorption under all-sky conditions have a higher effect than the estimated clear-sky SSR trends (see table 1) and the estimated effects of changes in clouds cover (see CCRE in table 1), and are more consistent with the magnitude of the observed all-sky SSR trends (presented in table 1). Thus, these results suggest that the increase in atmospheric absorption was the strongest contributor for the negative SSR trends observed in these four composites in north and northeast Brazil, with contributions also from changes in cloud cover. The difference in the all-sky and clear-sky absorption trends at these four composites indicates that clouds played an important role in the increasing in absorption, most likely by enhancing the optical path of photons via multiple scattering under partially cloudy conditions. The



589 results also suggest that these changes in atmospheric absorption were greatly influenced by the
590 changes in the optical properties of the aerosols present in these regions. Our results showed the
591 occurrence of increasing anthropogenic emissions of SO₂ and black carbon, which did not seem to
592 significantly change the AOD (possibly because of its competing effects with the reduction of
593 biomass burning emissions in South Amazon), but increased the AAOD. This is most likely the cause
594 for the increase in atmospheric absorption at the four composites. All of this points to a relevant
595 influence of anthropogenic factors to the SSR trends in the first two decades of the 21st century in the
596 regions around Manaus, Belem, Fortaleza and Salvador. Remembering that these are all big cities
597 with over a million inhabitants each, therefore this result could be biased towards big population
598 centers.

599 **4.3 Midwest and Southeast Brazil**

600 In this section we discuss the causes of the decadal SSR trends in the Middle West and
601 Southeast Brazil composites. Both all-sky SSR composites show near-zero trends, with -0.4 ± 2.7 W/
602 m² per decade in the Middle West and -0.6 ± 5.4 W/m² per decade in Southeast Brazil in the first two
603 decades of the 21st century. Both composites show clear-sky SSR dimming (statistically significant in
604 the Middle West and statistically insignificant in the Southeast) and statistically significant decrease in
605 cloud cover in the period. An increase in atmospheric absorption was also observed at these locations,
606 but the trends were substantially smaller than the trends observed in the four composites discussed in
607 the previous section. These results already suggest different physical processes playing a role in the
608 causes of SSR decadal trends in these regions.

609 The trends in fractional clear-sky atmospheric absorption in the two composites are similar to
610 each other (0.0051 ± 0.005 per decade in the Middle West and 0.0059 ± 0.007 per decade in the
611 Southeast) and are larger than the trends in three out of the four composites discussed in the previous
612 section. The clear-sky absorption trends are also larger than the all-sky absorption trends in the
613 Middle West and Southeast. This indicates a bigger relative relevance of the cloud-free processes for
614 the SSR trends in these two regions compared to the four locations previously discussed. This is
615 reinforced by the clear-sky SSR dimming at the two locations, and is also most likely associated with
616 increasing anthropogenic emissions, which lead to more absorptive aerosols, without significant
617 change in AOD.

618 A comparison between the results of these two composites with the four composites in North
619 and Northeast Brazil supports the discussion regarding the impacts of broken clouds to the solar
620 atmospheric absorption and the distribution of cloud cover occurrences, presented in the previous
621 section. As discussed by Reboita et al. (2010) and by Ferreira and Reboita (2022), in the region from
622 Middle West to Southeastern Brazil a stronger influence of large scale synoptic meteorological
623 systems like cold fronts, South Atlantic Convergence Zone (SACZ) and the South American Low
624 Level Jet (SALLJ) contrasts with Northern and Northeastern Brazil, where local convection and
625 circulation play a more important role. This leads to different precipitation and cloudiness regimes
626 between the composites discussed in this section and in previous section. These regimes magnify the



627 effects of atmospheric absorption in the North and Northeastern Brazil, again fitting to the results by
628 Li et al. (1995), while not doing so in the rest of the country.

629 The results of these two composites also show a significant positive effect of changes in cloud
630 cover on the SSR trends. Strong significant negative trends in cloud cover were observed at both
631 regions. As a result of the competing effects between cloud-free processes and changes in cloud cover,
632 the resulting SSR trends in the first two decades of the 21st century were negative, but near-zero, for
633 both composites. This shows opposing effects of anthropogenic (changes in aerosols) and natural
634 (changes in cloud cover) changes canceling out.

635 **4.4 South Amazon and South Brazil**

636 In this section we discuss the causes for the SSR decadal trends in the South Amazon and
637 South Brazil. In both regions statistically insignificant brightening was observed in the all-sky SSR
638 trends. Clear-sky SSR trends also showed brightening (statistically insignificant) in both regions.
639 Cloud cover trends in South Brazil were rather small (-0.4 [-1.4 ; 0.6] % per decade), while cloud data
640 was not available for South Amazon.

641 For the South Amazon, the most relevant aspect to be discussed is the strong negative trend in
642 AOD observed in the study period, associated with the documented reduction in deforestation and
643 biomass burning in the Amazon (Silva Junior et al., 2021). Amazon biomass burning aerosols play an
644 important role in the atmospheric transmissivity in the region, but their emission, and consequently
645 their effects, are highly seasonally dependent, as shown by Schwarz et al. (2019). For this reason,
646 even though the annual AOD decadal trends show very strong negative values, the strong effects on
647 SSR are present mostly in the dry season (southern hemisphere winter), and are smoothed out with
648 annual means and decadal trends calculations. The seasonal clear-sky SSR trends in this composite
649 are positive (statistically insignificant at the 95% confidence level) in winter and spring (5.0 ± 5.6 and
650 1.1 ± 3.9 W/m² per decade, respectively) and negative (statistically insignificant at the 95%
651 confidence level) in summer and fall (-2.6 ± 2.7 and -1.6 ± 3.3 W/m² per decade, respectively),
652 reinforcing this hypothesis. This smoothing of the AOD effects in the annual means and decadal
653 trends is most likely the reason why, despite the strong negative AOD trends in the region, the all-sky
654 and clear-sky SSR trends show positive trends with an absolute magnitude remarkably smaller than
655 the trends observed in north and northeastern Brazil. This counterintuitive result (strong negative
656 AOD decadal trend not resulting in strong brightening) reveals the importance of taking seasonality
657 into account when investigating the response of SSR to changes in AOD.

658 In South Brazil, the SSR decadal trends are weakly positive, not of statistical significance,
659 both under all-sky and clear-sky conditions. This suggests the lack of a strong driver for the SSR
660 trends in the period analyzed. Cloud cover shows a small negative trend (statistically insignificant).
661 Near-zero trends are also found in AOD and in atmospheric absorption. The map of AAOD at 500 nm
662 shows small positive trends in the period, but water vapour shows small negative trends. It is
663 important to note that due to the logarithmic response of atmospheric absorption to changes in water
664 vapour (e.g. Hakuba et al., 2016), this is the region in Brazil with the expected strongest sensitivity to



665 changes in water vapour. Combining all these results together denotes competing small effects from
666 different sources, and this is most likely the reason for the resulting non significant trend observed.
667 Another relevant aspect to be highlighted, is that the period of analysis did not show a strong
668 transition in the signal from oceanic modes in the Atlantic. Chtirkova et al. (2023) pointed out the
669 importance of the AMM and AMO oceanic modes for the SSR trends in South America. This could be
670 relevant for all composites, but the lack of strong effects on SSR changes of the existing forcing
671 elements in South Brazil in the post 2000 period let us to hypothesize that in a transitional period of
672 AMM and/or AMO, internal variability could dominate the SSR trends in this region, especially via
673 changes in cloud cover. This hypothesis is reinforced by the cloud cover trends from ERA5 for the
674 1990-2006 period (Figure A1, in appendix), which show strong negative cloud cover trends in the
675 region associated with the transitioning of the AMO from a negative to a positive phase. The
676 expectation is that the cloud cover trends in this period dominated the SSR trends, causing brightening
677 in the last decade of the 20st century in South Brazil. However, the lack of SSR data before 2000 did
678 not allow us to verify this hypothesis.

679 **5. Conclusions**

680 In this study we presented and investigated the magnitudes of the SSR trends and their
681 associated causes over the first two decades of the 21st century based on 34 stations in Brazil, divided
682 into 8 composites of 3 to 5 stations each. These are: Manaus region, Belem region, South Amazon,
683 Fortaleza region, Middle west, Salvador region, Southeast Brazil and South Brazil. The exact
684 temporal coverage of the SSR time series was composite-dependent, covering 22 years (2001-2022)
685 in the four southernmost composites (South, Southeast, Middle West and Salvador), and only 14 years
686 (2008-2021) in the South Amazon composite, the shortest time spam of all composites in this study.
687 We used cloud cover data from in situ measurements, clear-sky time series derived with two different
688 methods (using Synop cloud cover and using the method by Correa et al., 2022), atmospheric
689 absorption calculated combining in situ and satellite measurements, AOD from the CAMS reanalysis,
690 AAOD from OMI satellite observations and anthropogenic emissions from EDGAR to investigate the
691 causes of the SSR trends in the eight composites in their period of data availability. Our results
692 showed that a strong dimming occurred in the composites located in north and northeast Brazil
693 (Manaus, Belem, Fortaleza and Salvador) in the period of study, while the other four composites all
694 showed statistically insignificant trends (positive in the South Amazon and South Brazil, and negative
695 in the Southeast and Midwest). A deeper analysis on the causes of the trends revealed significant
696 contributions of both clear-sky and cloud cover changes to the trends observed in the north and
697 northeast Brazil, but with a dominance of the effects of increasing atmospheric absorption under all-
698 sky conditions. Previous studies (e.g, Li et al., 1995; Byrne et al., 1996) have discussed the increase in
699 atmospheric absorption under broken cloud conditions due to the multiple scattering by clouds and
700 absorption by water vapour and aerosols. In the case of north and northeast Brazil, we believe that this
701 is associated with an increase in absorption possibly by aerosols, also responsible for a clear-sky SSR



27

702 dimming, and the characteristics of cloud occurrence in those regions. The massive occurrence of
703 partially cloudy conditions at these regions, in comparison with the other composites analysed in this
704 study, make this mechanism much more relevant at the North and Northeast Brazil stations than in all
705 of the others. In Southeast and Middle West Brazil, statistically insignificant negative SSR trends in
706 the period were most likely the results of competing effects of negative cloud cover trends (resulting
707 in a positive forcing on all-sky SSR) and negative clear-sky SSR trends (resulting in a negative
708 forcing on all-sky SSR), where the clear-sky trends are also most likely associated with changes in
709 aerosol absorption. In the South Amazon the signal of the strong aerosol reduction, resulting from the
710 reduction in biomass burning in the Amazon at the beginning of the 21st century (Silva Junior et al.,
711 2021), dominated the observed brightening. But due to the strong seasonality of the biomass burning
712 in the Amazon (Schwarz et al., 2019), the resulting trend was statistically insignificant. Finally in
713 South Brazil, competing minor effects of cloud-free processes and cloud cover changes resulted in
714 statistically insignificant brightening. This study contributes to the understanding of the causes of SSR
715 decadal trends in a world region with still limited observational data, and opens space for further
716 research on the climate effects of such trends.

717 **Data availability**

718 The data from the IAG/USP station can be requested at http://www.estacao.iag.usp.br/sol_dados.php
719 (last access: 21 Feb 2024). The data from INMET stations can be requested at [https://
720 bdmep.inmet.gov.br/](https://bdmep.inmet.gov.br/) (last access: 21 Feb 2024). The BSRN SSR data is available at the BSRN
721 website ([https://
722 ceres.larc.nasa.gov/data/](https://bsrn.awi.de/)). The CERES products are available at the CERES website ([https://
724 cds.climate.copernicus.eu/cdsapp#!/dataset/reanalysis-era5-single-levels-monthly-means](https://
723 cds.climate.copernicus.eu/cdsapp#!/dataset/reanalysis-era5-single-levels-monthly-means) . The CAMS
725 AOD reanalysis data is available under [https://
727 www.ecmwf.int/en/research/climate-reanalysis/cams-
728 reanalysis](https://www.ecmwf.int/en/research/climate-reanalysis/cams-
726 reanalysis) . Data of anthropogenic emissions estimates is available at the EDGAR website ([https://
730 edgar.jrc.ec.europa.eu/emissions_data_and_maps](https://
729 edgar.jrc.ec.europa.eu/emissions_data_and_maps) , last access: 21 Feb 2024). The data from the OMI
731 instrument used in this study is available at [https://disc.gsfc.nasa.gov/datasets/OMAERUVd_003/
733 summary](https://disc.gsfc.nasa.gov/datasets/OMAERUVd_003/
732 summary) (last access 21 Feb 2024). The satellite cloud fraction data from CLARA, used to apply the
734 clear-sky method used in this study, can be found on the CM SAF website (<https://www.cmsaf.eu/>)
735 and downloaded using the Web User Interface at <https://wui.cmsaf.eu/>

731 **Author contributions**

732 LFC designed the study, organised the data and wrote the original manuscript. DF, BC and MW
733 revised and edited the text. All authors contributed to the analysis and to the final paper.

734 **Competing interests**

735 The authors declare that they have no conflict of interest.



736 **Acknowledgements**

737 This study was funded by the Swiss National Science Foundation grant no. 200020_188601.
738 The authors would like to thank the Instituto Nacional de Meteorologia (INMET) and the Weather
739 Station of the Institute of Astronomy, Geophysics and Atmospheric Science of the University of São
740 Paulo for providing the meteorological observations. We express our gratitude to the teams that
741 produce and maintain the high quality meteorological data used in this study, from BSRN, CERES,
742 ERA5, CAMS, OMI, EDGAR and CLARA.

743 **References**

- 744 Artaxo, P., Oliveira, P. H., Lara, L. L., Pauliquevis, T. M., Rizzo, L. V., Junior, C. P., ... &
745 Correia, A. L. (2006). Efeitos climáticos de partículas de aerossóis biogênicos e
746 emitidos em queimadas na Amazônia. *Revista brasileira de meteorologia*, 21(3a),
747 168-22.
- 748 Augustine, J. A., & Capotondi, A. (2022). Forcing for multidecadal surface solar radiation
749 trends over Northern Hemisphere continents. *Journal of Geophysical Research:*
750 *Atmospheres*, 127(16), e2021JD036342.
- 751 Byrne, R. N., Somerville, R. C. J., & Subaşılar, B. (1996). Broken-cloud enhancement of
752 solar radiation absorption. *Journal of Atmospheric Sciences*, 53(6), 878-886.
- 753 Chiacchio, M., & Wild, M. (2010). Influence of NAO and clouds on long-term seasonal
754 variations of surface solar radiation in Europe. *Journal of Geophysical Research:*
755 *Atmospheres*, 115(D10).
- 756 Chtirkova, B., Folini, D., Correa, L. F., & Wild, M. (2023). Internal variability of the climate
757 system mirrored in decadal-scale trends of surface solar radiation. *Journal of*
758 *Geophysical Research: Atmospheres*, e2023JD038573.
- 759 Correa, L. F., Folini, D., Chtirkova, B., & Wild, M. (2022). A Method for Clear-Sky
760 Identification and Long-Term Trends Assessment Using Daily Surface Solar
761 Radiation Records. *Earth and Space Science*, 9(8), e2021EA002197.
- 762 Crippa, M., Guizzardi, D., Muntean, M., Schaaf, E., Dentener, F., Van Aardenne, J. A., ... &
763 Janssens-Maenhout, G. (2018). Gridded emissions of air pollutants for the period
764 1970–2012 within EDGAR v4. 3.2. *Earth Syst. Sci. Data*, 10(4), 1987-2013.
- 765 Da Silva, V. D. P. R., e Silva, R. A., Cavalcanti, E. P., Braga, C. C., de Azevedo, P. V., Singh,
766 V. P., & Pereira, E. R. R. (2010). Trends in solar radiation in NCEP/NCAR database
767 and measurements in northeastern Brazil. *Solar Energy*, 84(10), 1852-1862.
- 768 de Jong, P., Barreto, T. B., Tanajura, C. A., Kouloukoui, D., Oliveira-Esquerre, K. P.,
769 Kiperstok, A., & Torres, E. A. (2019). Estimating the impact of climate change on
770 wind and solar energy in Brazil using a South American regional climate model.
771 *Renewable energy*, 141, 390-401.
- 772 de Lima, F. J. L., Martins, F. R., Costa, R. S., Gonçalves, A. R., dos Santos, A. P. P., &
773 Pereira, E. B. (2019). The seasonal variability and trends for the surface solar



- 774 irradiation in northeastern region of Brazil. *Sustainable Energy Technologies and*
775 *Assessments*, **35**, 335-346.
- 776 Doelling, D. R., Loeb, N. G., Keyes, D. F., Nordeen, M. L., Morstad, D., Nguyen, C., ... &
777 Sun, M. (2013). Geostationary enhanced temporal interpolation for CERES flux
778 products. *Journal of Atmospheric and Oceanic Technology*, **30**(6), 1072-1090.
- 779 Driemel, A., Augustine, J., Behrens, K., Colle, S., Cox, C., Cuevas-Agulló, E., ... & König-
780 Langlo, G. (2018). Baseline Surface Radiation Network (BSRN): structure and data
781 description (1992–2017). *Earth System Science Data*, **10**(3), 1491-1501.
- 782 Dutton, E. G., Stone, R. S., Nelson, D. W., & Mendonca, B. G. (1991). Recent interannual
783 variations in solar radiation, cloudiness, and surface temperature at the South Pole.
784 *Journal of Climate*, **4**(8), 848-858.
- 785 Ferreira, G. W., & Reboita, M. S. (2022). A new look into the South America precipitation
786 regimes: Observation and Forecast. *Atmosphere*, **13**(6), 873.
- 787 Fisch, G., MARENGO, J. A., & NOBRE, C. A. (1998). Uma revisão geral sobre o clima da
788 Amazônia. *Acta amazônica*, **28**, 101-101.
- 789 Gilgen, H., Roesch, A., Wild, M., & Ohmura, A. (2009). Decadal changes in shortwave
790 irradiance at the surface in the period from 1960 to 2000 estimated from Global
791 Energy Balance Archive Data. *Journal of Geophysical research: atmospheres*,
792 **114**(D10).
- 793 Hakuba, M. Z., Folini, D., & Wild, M. (2016). On the zonal near-constancy of fractional solar
794 absorption in the atmosphere. *Journal of Climate*, **29**(9), 3423-3440.
- 795 Hersbach, H., Bell, B., Berrisford, P., Hirahara, S., Horányi, A., Muñoz-Sabater, J., ... &
796 Thépaut, J. N. (2020). The ERA5 global reanalysis. *Quarterly Journal of the Royal*
797 *Meteorological Society*, **146**(730), 1999-2049.
- 798 IBGE. Censo Demográfico. Rio de Janeiro, Brazil: Fundação Instituto Brasileiro de
799 Geografia e Estatística. 2022. Available at: [https://censo2022.ibge.gov.br/panorama/](https://censo2022.ibge.gov.br/panorama/index.html)
800 [index.html](https://censo2022.ibge.gov.br/panorama/index.html) Last access: 01 Nov. 2023. [https://censo2022.ibge.gov.br/panorama/](https://censo2022.ibge.gov.br/panorama/index.html)
801 [index.html](https://censo2022.ibge.gov.br/panorama/index.html)
- 802 Inness, A., Ades, M., Agustí-Panareda, A., Barré, J., Benedictow, A., Blechschmidt, A. M., ...
803 & Suttie, M. (2019). The CAMS reanalysis of atmospheric composition.
804 *Atmospheric Chemistry and Physics*, **19**(6), 3515-3556.
- 805 Kambezidis, H. D., Kaskaoutis, D. G., Kharol, S. K., Moorthy, K. K., Satheesh, S. K.,
806 Kalapureddy, M. C. R., ... & Wild, M. (2012). Multi-decadal variation of the net
807 downward shortwave radiation over south Asia: The solar dimming effect.
808 *Atmospheric Environment*, **50**, 360-372.
- 809 Kendall, M. G. (1975). Rank correlation methods. 2nd impression. *Charles Griffin and*
810 *Company Ltd. London and High Wycombe*.
- 811 Kudo, R., Uchiyama, A., Ijima, O., Ohkawara, N., & Ohta, S. (2012). Aerosol impact on the
812 brightening in Japan. *Journal of Geophysical Research: Atmospheres*, **117**(D7).
- 813 Li, Z., Barker, H. W., & Moreau, L. (1995). The variable effect of clouds on atmospheric
814 absorption of solar radiation. *Nature*, **376**(6540), 486-490.



- 815 Lobo, C., & Cunha, J. M. P. D. (2019). Migração e mobilidade pendular nas áreas de
816 influência de metrópoles brasileiras. *Mercator (Fortaleza)*, 18.
- 817 Loeb, N. G., Doelling, D. R., Wang, H., Su, W., Nguyen, C., Corbett, J. G., ... & Kato, S.
818 (2018). Clouds and the earth's radiant energy system (CERES) energy balanced and
819 filled (EBAF) top-of-atmosphere (TOA) edition-4.0 data product. *Journal of*
820 *Climate*, 31(2), 895-918.
- 821 Long, C. N., & Dutton, E. G. (2002). BSRN Global Network Recommended QC Tests, V2. 0,
822 BSRN Technical Report.
- 823 Long, C. N., Dutton, E. G., Augustine, J. A., Wiscombe, W., Wild, M., McFarlane, S. A., &
824 Flynn, C. J. (2009). Significant decadal brightening of downwelling shortwave in the
825 continental United States. *Journal of Geophysical Research: Atmospheres*,
826 114(D10).
- 827 Madhavan, B. L., Deneke, H., Witthuhn, J., & Macke, A. (2017). Multiresolution analysis of
828 the spatiotemporal variability in global radiation observed by a dense network of 99
829 pyranometers. *Atmospheric Chemistry and Physics*, 17(5), 3317-3338.
- 830 Mann, H. B. (1945). Nonparametric tests against trend. *Econometrica: Journal of the*
831 *econometric society*, 245-259.
- 832 Nishizawa, S., & Yoden, S. (2005). Distribution functions of a spurious trend in a finite
833 length data set with natural variability: Statistical considerations and a numerical
834 experiment with a global circulation model. *Journal of Geophysical Research:*
835 *Atmospheres*, 110(D12).
- 836 Norris, J. R., & Wild, M. (2007). Trends in aerosol radiative effects over Europe inferred
837 from observed cloud cover, solar "dimming," and solar "brightening". *Journal of*
838 *Geophysical Research: Atmospheres*, 112(D8).
- 839 Ohmura, A., & Lang, H. (1989). Secular variation of global radiation over Europe, in Current
840 Problems in Atmospheric Radiation. *edited by J. Lenoble, & JF Geleyn*, 98, 301.
- 841 Ohmura, A., Dutton, E. G., Forgan, B., Fröhlich, C., Gilgen, H., Hegner, H., ... & Wild, M.
842 (1998). Baseline Surface Radiation Network (BSRN/WCRP): New precision
843 radiometry for climate research. *Bulletin of the American Meteorological Society*,
844 79(10), 2115-2136.
- 845 Ohmura, A. (2009). Observed decadal variations in surface solar radiation and their causes.
846 *Journal of Geophysical Research: Atmospheres*, 114(D10).
- 847 Pfeifroth, U., Sanchez-Lorenzo, A., Manara, V., Trentmann, J., & Hollmann, R. (2018).
848 Trends and variability of surface solar radiation in Europe based on surface-and
849 satellite-based data records. *Journal of Geophysical Research: Atmospheres*,
850 123(3), 1735-1754.
- 851 Raichijk, C. (2012). Observed trends in sunshine duration over South America. *International*
852 *Journal of Climatology*, 32(5), 669-680.
- 853 Reboita, M. S., Gan, M. A., Da Rocha, R. P., & Ambrizzi, T. (2010). Precipitation regimes in
854 South America: a bibliography review. *Revista Brasileira de Meteorologia*, 25(2),
855 185-204.



- 856 Russak, V. (1990). Trends of solar radiation, cloudiness and atmospheric transparency during
857 recent decades in Estonia. *Tellus B*, 42(2), 206-210.
- 858 Schwartz, R. D. (2005). Global dimming: Clear-sky atmospheric transmission from
859 astronomical extinction measurements. *Journal of Geophysical Research:
860 Atmospheres*, 110(D14).
- 861 Schwarz, M., Folini, D., Hakuba, M. Z., & Wild, M. (2018). From point to area: Worldwide
862 assessment of the representativeness of monthly surface solar radiation records.
863 *Journal of Geophysical Research: Atmospheres*, 123(24), 13-857.
- 864 Schwarz, M., Folini, D., Yang, S., & Wild, M. (2019). The annual cycle of fractional
865 atmospheric shortwave absorption in observations and models: spatial structure,
866 magnitude, and timing. *Journal of Climate*, 32(20), 6729-6748.
- 867 Sen, P. K. (1968). Estimates of the regression coefficient based on Kendall's tau. *Journal of
868 the American statistical association*, 63(324), 1379-1389.
- 869 Silva Junior, C. H., Pessôa, A. C., Carvalho, N. S., Reis, J. B., Anderson, L. O., & Aragão, L.
870 E. (2021). The Brazilian Amazon deforestation rate in 2020 is the greatest of the
871 decade. *Nature ecology & evolution*, 5(2), 144-145.
- 872 Stjern, C. W., Kristjánsson, J. E., & Hansen, A. W. (2009). Global dimming and global
873 brightening—An analysis of surface radiation and cloud cover data in northern
874 Europe. *International Journal of Climatology: A Journal of the Royal
875 Meteorological Society*, 29(5), 643-653.
- 876 Torres, O., Tanskanen, A., Veihelmann, B., Ahn, C., Braak, R., Bhartia, P. K., ... & Levelt, P.
877 (2007). Aerosols and surface UV products from Ozone Monitoring Instrument
878 observations: An overview. *Journal of Geophysical Research: Atmospheres*,
879 112(D24).
- 880 Vera, C., Baez, J., Douglas, M., Emmanuel, C. B., Marengo, J., Meitin, J., ... & Zipser, E.
881 (2006). The South American low-level jet experiment. *Bulletin of the American
882 Meteorological Society*, 87(1), 63-78.
- 883 Wang, C., Jeong, G. R., & Mahowald, N. (2009). Particulate absorption of solar radiation:
884 anthropogenic aerosols vs. dust. *Atmospheric Chemistry and Physics*, 9(12),
885 3935-3945.
- 886 Wild, M. (2009). Global dimming and brightening: A review. *Journal of Geophysical
887 Research: Atmospheres*, 114(D10).
- 888 Wild, M., Wacker, S., Yang, S., & Sanchez-Lorenzo, A. (2021). Evidence for clear-sky
889 dimming and brightening in central Europe. *Geophysical Research Letters*, 48(6),
890 e2020GL092216.
- 891 Yamasoe, M. A., Rosário, N. M. É., Almeida, S. N. S. M., & Wild, M. (2021). Fifty-six years
892 of surface solar radiation and sunshine duration over São Paulo, Brazil: 1961–2016.
893 *Atmospheric Chemistry and Physics*, 21(9), 6593-6603.
- 894 Yang, S., Wang, X. L., & Wild, M. (2018). Homogenization and trend analysis of the 1958–
895 2016 in situ surface solar radiation records in China. *Journal of Climate*, 31(11),
896 4529-4541.



32

897 Yuan, M., Leirvik, T., & Wild, M. (2021). Global trends in downward surface solar radiation
 898 from spatial interpolated ground observations during 1961–2019. *Journal of*
 899 *Climate*, 34(23), 9501-9521.

900 Zuluaga, C. F., Avila-Diaz, A., Justino, F. B., & Wilson, A. B. (2021). Climatology and trends
 901 of downward shortwave radiation over Brazil. *Atmospheric Research*, 250,
 902 105347.

903 **Appendix**

Station	Composite	Coordinates	Does it include SYNOP cloud cover?
Manaus	Manaus region	3.10S 60.01W	yes
Coari	Manaus region	4.10S 63.14W	yes
Rio Urubu	Manaus region	2.63S 59.60W	no
Urucará	Manaus region	2.53S 57.75W	no
Belém	Belém region	1.41S 48.43W	yes
Castanhal	Belém region	1.30S 47.94W	no
Tucuruí	Belém region	3.82S 49.67W	yes
Salinópolis	Belém region	0.62S 47.35W	no
Alta Floresta	South Amazon	10.07S 56.17W	no
Ariquemes	South Amazon	9.94S 62.96W	no
Juína	South Amazon	11.37S 58.77W	no
Porto Velho	South Amazon	8.79S 63.84W	no
Sorriso	South Amazon	12.55S 55.72W	no
Fortaleza	Fortaleza region	3.81S 38.53W	yes
Areia	Fortaleza region	6.97S 35.71W	yes
Caicó	Fortaleza region	6.46S 37.08W	yes
Natal	Fortaleza region	5.83S 35.20W	yes
Brasília	Midwest	15.78S 47.92W	yes
Goiânia	Midwest	16.64S 49.22W	yes
Campo Grande	Midwest	20.44S 54.72W	yes
Salvador	Salvador region	13.00S 38.50W	yes
Cruz das Almas	Salvador region	12.67S 39.08W	yes
Feira de Santana	Salvador region	12.19S 38.96W	yes
Itirucu	Salvador region	13.52S 40.11W	yes
Curitiba	South	25.44S 49.23W	yes
Porto Alegre	South	30.05S 51.17W	yes



Santa Maria	South	29.72S 53.72W	yes
Florianópolis*	South	27.60S 48.52W	yes
Campos do Jordão	Southeast	22.75S 45.60W	yes
Monte Verde	Southeast	22.86S 46.04W	no
Rio de Janeiro - Marambaia	Southeast	23.05S 43.59W	yes
Seropédica	Southeast	22.75S 43.68W	no
São Paulo*	Southeast	23.65S 46.62W	yes

904

905

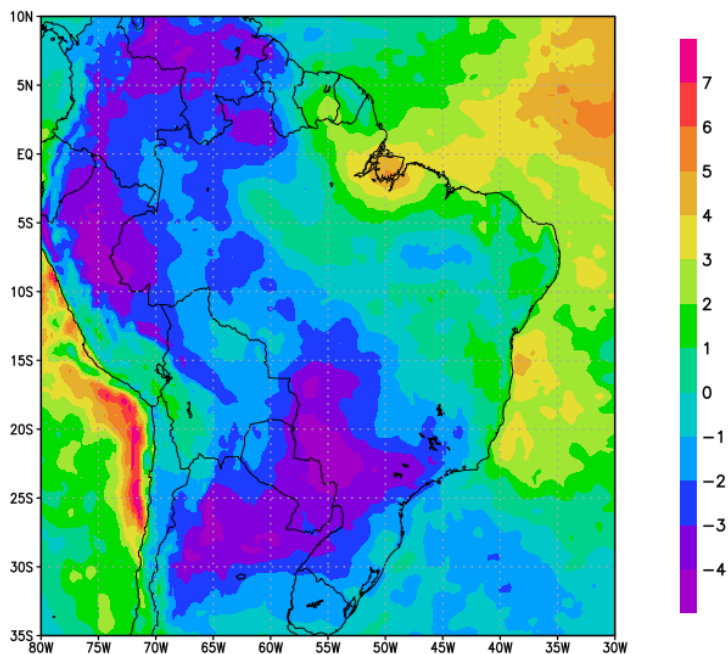
906

907

908

909

Table A1: Stations used in the study, the composites they were associated with, their coordinates and information whether Synop cloud cover data was available. *Stations not from the Brazilian National Institute of Meteorology. Florianópolis station from BSRN; São Paulo station from the Institute for Astronomy, Geophysics and Atmospheric Sciences at the University of São Paulo.



910

911

Figure A1 - Total cloud cover trends for the 1990-2006 period (in % per decade) from ERA5.